Universal relative scaling of longitudinal structure functions in shear-dominated turbulence

K.R. Maryada[1,†], **S.W. Armfield**[2], **M. MacDonald**[1], **P. Dhopade**[1] **and S.E. Norris**[1]

[1]Department of Mechanical and Mechatronics Engineering, The University of Auckland, Auckland 1010, New Zealand

[2]School of Aerospace, Mechanical and Mechatronic Engineering, The University of Sydney, New South Wales 2006, Australia

Shear significantly influences turbulence in the energy-containing range of shear-dominated flows, and the longitudinal structure functions do not have a universal form as they do in homogeneous isotropic turbulence. Despite this, the relative scaling of structure functions exhibits universal sub-Gaussian behaviour in shear-dominated flows, in particular for turbulent boundary layers, channels and Taylor–Couette flows. Our investigation of a turbulent vertical buoyancy layer at $Pr = 0.71$ using direct numerical simulation shows this universality even in moderate-Reynolds-number buoyancy-driven but shear-dominated boundary layers. It is demonstrated that the universality is related to the energy density of the eddies, which attains a hierarchical equilibrium in the energy-containing range of shear-dominated turbulence. We conjecture that the universal sub-Gaussian behaviour of the energy density of the energy-containing range, which was considered to be non-trivial in prior studies, is related to the universal anomalous scaling exponents of the inertial subrange turbulence. Based on this conjecture, we propose a hypothesis that relates large-scale eddies and the intermittent dissipation field in shear-dominated turbulence, highlighting a relationship between large and small scales. A phenomenological model is also developed to predict the scaling, which is verified using data from a turbulent boundary layer, half-channel and vertical buoyancy layer at friction Reynolds numbers spanning four orders of magnitude. Excellent agreement is observed.

Key words: turbulence theory, turbulent boundary layers

† Email address for correspondence: kmar699@aucklanduni.ac.nz

1. Introduction

The scaling of turbulent flows has intrigued researchers for over a century, as understanding the scaling would pave the way for a unified theory of turbulence. One of the most influential works in this regard is the theory of Kolmogorov (1941) on homogeneous isotropic turbulence. In large-Reynolds-number (Re) flows, at scales where viscosity and integral length scales are insignificant (the inertial subrange), eddies with length scale l only depend on the turbulent dissipation rate ϵ. These eddies are significantly larger than the Kolmogorov microscale; therefore, the dissipation effects are insignificant. According to Kolmogorov (1941), at these scales, in homogeneous isotropic turbulence, the structure functions (a proxy for turbulent eddies) of different orders scale as

$$S_n = \langle |u(x + r) - u(x)|^n \rangle = C_n (\epsilon r)^{n/3}, \qquad (1.1)$$

where u is the velocity field subtracted from the mean, x is the longitudinal coordinate, r is the separation distance and is representative of length scale l, C_n is a constant, which is not necessarily universal for different flows (Sreenivasan & Antonia 1997), and n is the order of the structure function. All the relevant quantities are ensemble-averaged unless specified. Throughout this paper, we use x, y and z to represent the streamwise, spanwise and wall-normal directions, respectively.

In homogeneous isotropic turbulence, it has since been known that S_n significantly deviates from (1.1), especially for $n > 3$, and this has been referred to as intermittency. This is due to the nature of ϵ, which is not uniform but has intermittent regions of ϵ significantly different from the mean. Essentially, $S_n \propto r^{\zeta_n}$ instead of $S_n \propto r^{n/3}$ as in (1.1). Here, ζ_n is often called the anomalous scaling exponent. Consequently, several phenomenological models have been proposed to predict ζ_n (Kolmogorov 1962; Frisch, Sulem & Nelkin 1978; Meneveau & Sreenivasan 1987; She & Leveque 1994). A major assumption in all these models is that turbulence in the inertial subrange can be modelled as a random multiplicative process.

Even in real-world shear-driven flows having significant large-scale anisotropy, the inertial subrange scaling ($S_n \propto r^{\zeta_n}$) is recovered at small scales, i.e. at scales smaller than the Corrsin length scale (Corrsin 1958) but larger than the Kolmogorov microscale (Arneodo *et al.* 1996; Toschi *et al.* 1999; Toschi, Leveque & Ruiz-Chavarria 2000; Gualtieri *et al.* 2002; Casciola *et al.* 2005; Attili & Bisetti 2012). This implies that the small scales (inertial subrange) in shear-driven flows scale similarly to homogeneous isotropic turbulence despite large-scale anisotropy. This result was also verified by de Silva *et al.* (2015) using high-Re datasets of atmospheric and turbulent boundary layers.

However, the scaling of large-scale eddies is less certain. The exponents ζ_n of the inertial subrange are not expected to hold at scales where the outer length scales of a system are comparable to r. Even external forces such as shear, buoyancy and stratification are expected to alter the scaling properties of the integral-scale motions. In most engineering flows, shear is almost always present and cannot be ignored. The variation of ζ_n is significant when shear is present, and several corrections have been proposed to predict the scaling of the structure functions under the assumption that a power-law scaling holds (Benzi *et al.* 1999; Toschi *et al.* 1999, 2000; Casciola *et al.* 2001, 2003, 2005; Gualtieri *et al.* 2002). However, the power-law scaling of large-scale eddies is not unequivocal. Recent studies of turbulent boundary layers, channels and pipes at high Re have shown that the power-law scaling of structure functions is not always observed at large scales (Davidson, Krogstad & Nickels 2006*a*; Davidson, Nickels & Krogstad 2006*b*; Davidson & Krogstad 2009, 2014; Chung *et al.* 2015*b*; de Silva *et al.* 2015, 2017; Pan & Chamecki

2016; Yang, Marusic & Meneveau 2016; Agostini & Leschziner 2017; Chamecki *et al.* 2017; Krug *et al.* 2017; Ghannam *et al.* 2018; Xie *et al.* 2021).

A different approach is to assume that at large scales, as the correlation between the eddies is weak, turbulence can be approximated as an additive process rather than multiplicative as assumed at small scales (Townsend 1976; Perry, Henbest & Chong 1986; Jiménez 1998; Mouri *et al.* 2006; Mouri, Hori & Takaoka 2009). This assumption regarding turbulence at energy-containing scales, especially for turbulent boundary layers and channels (Davidson *et al.* 2006*b*; Yang *et al.* 2016; Agostini & Leschziner 2017; Marusic & Monty 2019), has received renewed interest in the past few years. Under this assumption, the turbulence at scale *r* is statistically modelled as increments of eddies (addends) that are identically and independently distributed. Conceptually, this is similar to the model of Tennekes & Lumley (1972) and Jiménez (1998), which the authors formalised in the spectral domain. This assumption regarding turbulence at large scales can be used to explain scaling laws in the energy-containing range that are different from power-law scaling (Davidson *et al.* 2006*b*; Chung *et al.* 2015*b*; de Silva *et al.* 2015; Yang *et al.* 2016; Agostini & Leschziner 2017; Krug *et al.* 2017; Marusic & Monty 2019).

As the large scales can be approximated as a random additive process, turbulence at the energy-containing scales is expected to be Gaussian under the central limit theorem. However, it is well known that the energy-containing eddies in shear-dominated turbulence exhibit sub-Gaussian scaling behaviour (Jiménez 1998; Meneveau & Marusic 2013; Stevens, Wilczek & Meneveau 2014; de Silva *et al.* 2015, 2017; Krug *et al.* 2017). Recently, based on experimental and numerical data, it has been demonstrated that the even-order structure functions in turbulent boundary layers, channels and Taylor–Couette flows exhibit non-trivial but universal sub-Gaussian scaling behaviour (de Silva *et al.* 2015, 2017; Krug *et al.* 2017). However, it is not clear why this particular form of scaling is observed. The physical basis for the sub-Gaussian scaling is not understood, and it is not apparent how intermittency affects the scaling (Davidson & Krogstad 2014; de Silva *et al.* 2017).

It is evident from the above discussion that our understanding of the scaling of large-scale eddies in shear-dominated turbulence, especially structure functions of different orders, is far from complete, which forms the primary motivation of the current study. Here, we demonstrate that the energy ratio of the large-scale eddies in shear-dominated turbulence is universal, which is different from the universality observed in the scaling exponents of the inertial subrange. We then show that the universal scaling of the energy ratio of the energy-containing range is related to the scaling of the intermittent dissipation field in shear-dominated flows, which has been hitherto undetected and is one of the novel aspects of the current study. Notably, we establish that the sub-Gaussian scaling of the structure functions, which has been thought to be non-trivial in previous studies (Krug *et al.* 2017; de Silva *et al.* 2017), is related to the anomalous scaling of inertial subrange turbulence, providing a crucial link between large-scale eddies and the highly intermittent turbulent dissipation. Further, we propose a phenomenological model that sheds light on large-scale/small-scale interactions in shear-dominated turbulence while accurately predicting the energy ratio for low-order and high-order structure functions. The current results can form the basis for a theoretical framework that unites small and large scales in shear-dominated turbulence.

The paper is organised as follows. The hypothesis and the phenomenological model are described in § 2. An overview of the different numerical and experimental datasets used in the current study is given in § 3. To ensure that the hypothesis is not limited by low-Reynolds-number behaviour, we have investigated numerical and experimental datasets of three different shear-dominated flows across friction Reynolds numbers

$(Re_\tau = u_\tau \delta / \nu$, where u_τ is the friction velocity, δ is the outer length scale and ν is the kinematic viscosity) spanning four orders of magnitude. The proposed phenomenological model is validated in § 4 by investigating low-order and high-order structure functions, which account for the intense and rare fluctuations and those closer to the mean. Excellent agreement is observed between the data and the proposed model, with the percentage deviation being less than 10 %. The significance of the current theory with respect to canonical wall turbulence is also highlighted in this section. The conclusions are given in § 5.

2. Hierarchical energy equilibrium of the eddies

2.1. *Preliminaries*

We begin our analysis by considering eddies having scale $L_I < r < L_R$, where L_I ($L_I = \int_0^\infty R_{uu} \, \mathrm{d}x$, with R_{uu} being the two-point correlation in the streamwise direction) is the integral length scale and L_R is the location at which $R_{uu} \to 0$. While L_R imposes a strict upper limit on the range of statistically significant scales, it cannot be said that L_I is a strict lower bound. We assume that L_I imposes an upper bound on the multiplicative process, beyond which the additive process dominates (Mouri *et al.* 2006, 2009). Nevertheless, the exact values are not of concern as L_I and L_R are only characteristic scales. We use the terms energy-containing range and large scales to refer to this scaling range.

For $L_I < r < L_R$, we hypothesise that longitudinal structure functions of streamwise velocity fluctuations S_{2p} scale according to the ansatz

$$S_{2p}^{1/p} = K_{2p} \chi f(r) + M_{2p}. \tag{2.1}$$

Here, $p = n/2$ is the order, $S_{2p}^{1/p}$ is the normalised structure function, χ is a quantity of interest representing the eddies (elaborated below), K_{2p} and M_{2p} are constants (not universal for all turbulent flows) and r now corresponds to the non-dimensional separation distance. The $1/p$ power is chosen to ensure that $S_{2p}^{1/p}$ would always have the units of S_2, i.e. energy per unit mass. Equation (2.1) differs from (1.1) in that a power-law scaling is not explicitly assumed as $f(r)$ is an arbitrary function, which can vary for different flows. The exact functional form of $f(r)$ is unnecessary for the proposed scaling and is not predicted.

Equation (2.1) ensures the relation $S_2 = 2\langle uu \rangle (1 - R_{uu})$ is satisfied if $f(r) = 1 - R_{uu}$, $\chi = \langle uu \rangle$, $K_2 = 2$ and $M_2 = 0$ (Davidson *et al.* 2006*b*). The energy dissipation and streamwise velocity variance are related as $\langle uu \rangle \propto (\epsilon L_I)^{2/3}$ (Frisch 1995). In shear-dominated turbulence, $\langle uu \rangle \propto \langle uw \rangle$, where $\langle uw \rangle$ is the Reynolds shear stress. In the logarithmic region of turbulent boundary layers, $\langle uw \rangle \sim u_\tau^2$ (Townsend 1976; Perry *et al.* 1986; Marusic & Monty 2019). Equation (2.1) reduces to the following $\ln(r)$ law in turbulent boundary layers if $f(r) = \ln(r)$ and $\chi = u_\tau^2$ (Davidson *et al.* 2006*b*):

$$S_{2p}^{1/p} = A_p u_\tau^2 \ln(\hat{r}) + B_p, \tag{2.2}$$

where A_p and B_p are constants and $\hat{r}$, in this case, is normalised using the distance-from-the-wall scaling or the dissipation length scale (Townsend 1976; Perry *et al.* 1986; Davidson & Krogstad 2014; Pan & Chamecki 2016; Chamecki *et al.* 2017; Marusic & Monty 2019).

Therefore, χ in (2.1) can be replaced with any correlated quantity. Hence, for the rest of this paper, we focus on χ instead of making explicit references to ϵ, u_τ, $\langle uu \rangle$ and $\langle uw \rangle$.

We restrict ourselves to positive structure functions in this study. Also, we only work with absolute moments of structure functions as most phenomenological models for inertial subrange turbulence revolve around absolute moments (Kolmogorov 1962; Meneveau & Sreenivasan 1987; She & Leveque 1994). This also implies that the odd-order moments do not vanish even if the velocity fluctuations in the energy-containing range are assumed to be symmetric.

Along with structure functions, the 'energy-density' at scale r, which indicates the energy of eddies having size r, is another representative quantity of the eddies (Townsend 1976; Davidson *et al.* 2006*b*). It is defined as

$$E_p^r = r \frac{\partial S_{2p}^{1/p}}{\partial r}. \tag{2.3}$$

This relies on the observation that the ensembled averaged $S_{2p}^{1/p}$ is differentiable even if the eddies are modelled as discrete objects.

2.2. *Phenomenological model*

Turbulence, especially in the inertial subrange, is often conceptualised as eddies of different sizes/intensities organised hierarchically (Kolmogorov 1941, 1962; Meneveau & Sreenivasan 1987; She & Leveque 1994; Frisch 1995; Benzi *et al.* 1996; Ching *et al.* 2002; Jiang *et al.* 2006). Several studies of shear turbulence have postulated and observed hierarchical structures even in the energy-containing range (Townsend 1976; Perry *et al.* 1986; Yang *et al.* 2016; Dong *et al.* 2017; Marusic & Monty 2019; Motoori & Goto 2021). This paper also adopts the notion that the energy-containing eddies in shear turbulence exhibit hierarchical properties.

Also, let us assume that a normalised structure function (as shown in (2.1)) of order p indicates eddies having 'intensity' p (She & Leveque 1994; Frisch 1995). This would imply that high-order structure functions are indicative of rare and intense fluctuations, while low-order structure functions indicate fluctuations closer to the mean. This assumption is reasonable as high-order structure functions are related to the tails of the probability density functions (p.d.f.s) of velocity increments. In contrast, the low-order structure functions are related to the core of the p.d.f.s. Such an assumption was also made in the hierarchical structural model (HSM) of turbulence (She & Leveque 1994; She & Waymire 1995).

In a HSM, which is typically used to describe inertial subrange, it is assumed that the structure functions of different orders attain a hierarchical equilibrium (She & Leveque 1994; She & Waymire 1995; Benzi *et al.* 1996; Ching *et al.* 2002; Jiang *et al.* 2006). In this work, instead of focusing on structure functions themselves, we hypothesise that in shear-dominated turbulence, at the large scales where the additive process approximation holds, the energy of the eddies attains a 'hierarchical equilibrium' such that the energy of eddies of size r having intensity $p > 0$ is related to the energy of eddies of size r having intensity $m > 0$ as

$$\frac{E_p^r}{E_m^r} = F_{pm}, \tag{2.4}$$

where F_{pm} depends on p and m. Here, p and m refer to the order of the structure function ($p \neq m$). Here, F_{pm} indicates an underlying process in a statistical sense, and the instantaneous energy ratio need not be equal to F_{pm}. It is to be observed that the energy ratio of the eddies attains a hierarchical equilibrium and not the eddies themselves.

984 A28-5

For Gaussian statistics, F_{pm} can be written as

$$F_{pm} = \frac{E_p^r}{E_m^r} = G_{pm} = \pi^{((1/m-1/p)/2)} \frac{[\Gamma((2p+1)/2)]^{1/p}}{[\Gamma((2m+1)/2)]^{1/m}}, \quad (2.5)$$

where Γ is the Gamma function (Winkelbauer 2012). For even-order moments, this reduces to

$$F_{pm} = \frac{E_p^r}{E_m^r} = G_{pm} = \frac{[(2p-1)!!]^{1/p}}{[(2m-1)!!]^{1/m}}, \quad (2.6)$$

where !! is the double factorial (Krug *et al.* 2017).

We contend that F_{pm} is governed by processes that are not strictly Gaussian. This is based on several observations that revealed the sub-Gaussian nature of shear-dominated turbulence (Jiménez 1998; Meneveau & Marusic 2013; de Silva *et al.* 2015, 2017; Krug *et al.* 2017). The essence of this argument relies on the assumption that the non-Gaussian scaling of shear-dominated turbulence observed in previous studies is related to the non-Gaussian scaling of the energy ratio (verified in §§ 4.1 and 4.2, and discussed in § 4.4).

To account for this behaviour, we assume that two dominant processes govern the eddies' energy. One is a Gaussian process, and the other is a rare 'defect' event, which modulates turbulence. The phenomenology of defect events is qualitatively similar to the defect events of inertial subrange turbulence, which are responsible for the deviations from Kolmogorov (1941) scaling. In the energy-containing range, the primary effect of the defect events is to reduce the energy of the fluctuations and is responsible for deviations from Gaussian scaling. This, on phenomenological grounds, is expressed as $F_{pm} = G_{pm} W_{pm}$, with W_{pm} governing the defect events. In this formulation, W_{pm} is a correction term responsible for the non-Gaussian scaling. The rest of this section is dedicated to examining W_{pm}, as a model for W_{pm} allows us to quantify the deviation from the Gaussian scaling.

Kolmogorov (1941) postulated that the small scales are universal and are completely independent of the large scales. However, several studies since then have shown that the large scales of turbulence influence the small scales (e.g. Kolmogorov 1962; Obukhov 1962; Kraichnan 1974, 1991; Landau & Lifshitz 1987; Frisch 1995; Yeung, Brasseur & Wang 1995; Sreenivasan & Antonia 1997; Mouri *et al.* 2006, 2012). In inertial subrange turbulence, the influence of large scales on small scales is observed in the coefficients and not in the scaling exponents (Kraichnan 1974; Frisch *et al.* 1978; Frisch 1995; Sreenivasan & Antonia 1997), suggesting that despite the scaling exponents of the structure functions being universal, the large-scale structures affect the small scales. The influence of large scales on small scales has also been demonstrated in shear-driven flows (e.g. Mathis, Hutchins & Marusic 2009; Ganapathisubramani *et al.* 2012; Baars, Hutchins & Marusic 2016; Jacobi *et al.* 2021; Andreolli *et al.* 2023).

As large scales influence small scales, it is reasonable to assume that the large and small scales share the same signatures. This does not imply that the small scales dictate the properties of large scales but implies that large and small scales are related. In shear-dominated turbulence, we assume this signature is evident in the energy ratio of large-scale eddies. The inertial subrange scaling with intermittency corrections gives us information about small scales. Statistically, we postulate that the defect events in the energy-containing range are related to the defect events in the inertial subrange. Consequently, we include the anomalous scaling of the inertial subrange to model the large scales. Specifically, the distribution of the defect events in small scales is related to the distribution across large scales, implying that W_{pm} is a function of the

anomalous scaling exponents of the inertial subrange. Of course, the validity of this crucial assumption requires verification using numerical and experimental data, which we address in § 4.

Note that the inertial subrange scaling is recovered in shear-dominated turbulence at scales larger than the Kolmogorov microscale and smaller than the Corrsin length scale (Toschi *et al.* 1999; de Silva *et al.* 2015), suggesting that the above assumption on using the anomalous scaling of inertial subrange for small scales in shear-dominated turbulence is reasonable.

Based on the above arguments, we conjecture that (2.5) takes the following modified form:

$$F_{pm} = G_{pm}W_{pm} = G_{pm}\frac{\xi_p}{\xi_m} = \pi^{((1/m-1/p)/2)}\frac{[\Gamma((2p+1)/2)]^{1/p}}{[\Gamma((2m+1)/2)]^{1/m}}\frac{\xi_p}{\xi_m}, \qquad (2.7)$$

where ξ_p and ξ_m are the anomalous scaling exponents of normalised structure functions of inertial subrange. Here, $\xi_p = \zeta_n/p$ and $\xi_m = \zeta_n/m$.

In (2.7), we use the HSM to calculate the anomalous scaling exponents ξ_q ($q = p$ or m) (She & Leveque 1994):

$$\xi_q = \zeta_n/q = \left(\frac{n}{9} + 2\left[1 - \left(\frac{2}{3}\right)^{n/3}\right]\right)\Big/ q, \qquad (2.8)$$

where ζ_n is the formulation given by She & Leveque (1994). Also, ξ_q in (2.8) does not violate Novikov's inequality (Frisch 1995). This ensures $\xi_p/\xi_m < 1$ for all p and m so long as $p > m$. Therefore, F_{pm} in (2.7) would always exhibit sub-Gaussian behaviour.

Further, (2.8) can be decomposed as

$$\xi_q = \left(\frac{n}{3} + \tau_{n/3}\right)\Big/ q, \qquad (2.9a)$$

$$\tau_n = -\frac{2}{3}n + 2\left[1 - \left(\frac{2}{3}\right)^n\right], \qquad (2.9b)$$

with $n/3$ being the Kolmogorov (1941) prediction and τ_n being the intermittency correction (She & Leveque 1994; Frisch 1995).

From (2.5), (2.7) and (2.9), we see that Gaussian scaling is recovered if $\tau_n = 0$ (without any intermittency corrections) or if the dissipation is assumed to be uniform, as was done by Kolmogorov (1941). Note that it is the intermittent dissipation field that leads to anomalous scaling exponents in the inertial subrange (Kolmogorov 1962; Obukhov 1962; Frisch *et al.* 1978; Meneveau & Sreenivasan 1987; Dubrulle 1994; She & Leveque 1994; Frisch 1995; She & Waymire 1995; Benzi *et al.* 1996; Sreenivasan & Antonia 1997). This result is significant as it demonstrates that the departure from the Gaussian profile of the energy ratio of large-scale eddies in shear-dominated flows is directly related to the intermittency observed in inertial subrange turbulence of the same flow. Crucially, we use the anomalous scaling exponents of the inertial subrange to model the energy ratio of the large scales, highlighting a relationship between large and small scales. Note that we only use the characteristic scales (mentioned in § 2.1) to identify the range at which (2.7) holds. These are not exact numerical values as they depend on *Re*, the type of flow and the order of the structure function.

A natural consequence of the above conjecture and (2.7) and (2.9) is that the defect events in the energy-containing range are related to a Poisson distribution as ξ_q can be modelled using a Poisson process (Dubrulle 1994; She & Waymire 1995). This does not state that the inertial subrange and the energy-containing range defect events are the same.

It only suggests that these are related. Also, it is emphasised that this does not imply that the scaling of the energy ratio of large-scale eddies is similar to isotropic turbulence, as (2.7) is distinct from (1.1) with or without intermittency corrections.

Now, we comment on the signature of intermittency and universality at large scales in shear-dominated turbulence. In inertial subrange turbulence, it is known that the presence of hierarchical moments of turbulent dissipation is a signature of intermittency and universality (Dubrulle 1994; She & Leveque 1994; She & Waymire 1995; Benzi *et al.* 1996). At large scales, the signature of intermittency and universality is the hierarchical energy equilibrium of the eddies, leading to sub-Gaussian scaling. The present picture of sub-Gaussian scaling holds irrespective of the 'physical shape' of the eddies but only in the relative distribution of the energy across eddies of different intensities (the definition of energy ratio).

Note that when we refer to the intermittency of large scales, it is not related to the external intermittency observed in shear turbulence. In shear turbulence, external intermittency is often referred to as the turbulent/non-turbulent interface between the fully turbulent flow and the stationary/irrotational ambient (Chauhan, Philip & Marusic 2014; Gauding *et al.* 2021; Gustenyov *et al.* 2023).

The present scaling is not related to the SO(3) decomposition or the integral structure function scaling of shear turbulence. The SO(3) decomposition is primarily used to isolate turbulence's isotropic and anisotropic components (Arad, L'vov & Procaccia 1999; Biferale *et al.* 2002; Casciola *et al.* 2005). The integral structure function scaling predicts the scaling exponents by assuming that a power-law scaling exists (Toschi *et al.* 2000), which is unrelated to the present study. In this study, we work with normalised structure functions (2.1), and $f(r)$ is assumed to be an arbitrary function (see § 2.1 for details) and does not always have a power-law scaling (Davidson *et al.* 2006*b*; de Silva *et al.* 2015; Krug *et al.* 2017). It is stressed that this study investigates the energy ratio and does not examine the scaling exponents of inertial subrange turbulence. Also, this hypothesis differs from what is observed in the inertial subrange, where the structure functions exhibit generalised extended self-similarity, hierarchy and universality (Arneodo *et al.* 1996; Benzi *et al.* 1996; Ching *et al.* 2002; Jiang *et al.* 2006). Equation (2.7) differs from the (generalised) extended self-similarity formulation. In the present case, the energy ratio of the large-scale eddies of different orders attains universality even if the eddies themselves are not assumed to be universal.

3. Description of the numerical and experimental datasets

To verify the conjectured equation (2.7), we investigate the longitudinal structure functions in turbulent boundary layers (SLTEST, MBL1 and MBL2) using data from Kunkel & Marusic (2006), Hutchins *et al.* (2009), Baars *et al.* (2015, 2016), de Silva *et al.* (2015, 2017), turbulent half-channel flow (C590) of MacDonald (2022) and vertical buoyancy layers (N580 and N395). The datasets used in the current study are summarised in table 1.

SLTEST (Kunkel & Marusic 2006) corresponds to a field test, while MBL1 (Hutchins *et al.* 2009) and MBL2 (Baars *et al.* 2015, 2016) correspond to wind tunnel experiments at the University of Melbourne. The measurements were obtained using hot-wire anemometry, and further details are available in the relevant publications.

The relative scaling of longitudinal structure functions of SLTEST and MBL1 are from de Silva *et al.* (2017). For the MBL2 dataset (Baars *et al.* 2015, 2016), the longitudinal structure functions were calculated using Taylor's frozen turbulent hypothesis, akin to what is done by de Silva *et al.* (2015, 2017) and Krug *et al.* (2017).

Case	Flow	Reference	Technique	$\approx Re_\tau$
SLTEST	Atmospheric boundary layer	Kunkel & Marusic (2006)	Hot-wire	3×10^6
MBL1	Boundary layer	Hutchins *et al.* (2009)	Hot-wire	19 000
MBL2	Boundary layer	Baars *et al.* (2015, 2016)	Hot-wire	14 750
C590	Half-channel flow	MacDonald (2022)	DNS	590
N395	Vertical buoyancy layer	Present	DNS	395
N580	Vertical buoyancy layer	Present	DNS	580

Table 1. Summary of the experimental and numerical datasets.

We use direct numerical simulation (DNS) data for the half-channel flow and vertical buoyancy layer. The half-channel flow (C590) was simulated using a fourth-order staggered-grid finite-difference scheme described by Chung *et al.* (2015*a*). The reader is referred to MacDonald (2022) for additional details on numerical methods and boundary conditions. DNS of the vertical buoyancy layer (N395 and N580) was performed using an in-house second-order finite volume code (Armfield *et al.* 2003), which has been previously used to simulate turbulent natural convection (Maryada *et al.* 2023). Numerical simulations were performed at $Pr = 0.71$ using the non-dimensional governing equations and boundary conditions described by Maryada *et al.* (2023), and we refer the reader to the same paper for further details. The vertical buoyancy layer is a simplified representation of a vertical natural convection boundary layer immersed in a stably stratified medium (Giometto *et al.* 2017; Maryada *et al.* 2022, 2023). It is a buoyancy-driven flow (a model for vertical convection) in contrast to turbulent flat plate and channel flow boundary layers, which are driven by the momentum of the free stream or pressure differential.

To date, the structure functions of vertical buoyancy layers (vertical convection problems in general) have not been examined extensively, and it is not evident how similar or different these flows are when compared with canonical wall turbulence. In the general context of vertical convection, the vertical buoyancy layer investigated in this study is in the 'classical regime' and not the 'ultimate regime' (Ng *et al.* 2017; Ke *et al.* 2023; Maryada *et al.* 2023). In the classical regime, most of the turbulence is observed in the outer layer (wall-normal locations beyond the velocity maximum) and not close to the wall. This implies that the vertical buoyancy layer does not exhibit all the essential features of canonical wall turbulence (Ng *et al.* 2017; Ke *et al.* 2023), making it distinct from turbulent boundary layers and channels. Hence, it is examined in this study. We shall return to this flow configuration in § 4.3 where it is shown that the vertical buoyancy layer, despite its differences, exhibits the energy ratio universality of (2.7).

It is well known that high-order structure functions are prone to errors due to poor convergence. For SLTEST and MBL1, the convergence was verified until $2p = 10$ (de Silva *et al.* 2015). For MBL2 and DNS data, the convergence of the structure functions was checked using the methodology suggested by Huisman, Lohse & Sun (2013), Meneveau & Marusic (2013) and de Silva *et al.* (2015, 2017), and the data reported correspond to converged statistics (until $2p = 8$ for N580 and N395, and $2p = 6$ for C590 and MBL2 datasets). As a representative case, figure 1(*a*) shows the premultiplied p.d.f. of the velocity increment at $r^+ \approx 7000$ ($r^+ > L_I^+$) for the MBL2 dataset. The area under the curve in the figure is the moment, and the smoothness of the curve suggests convergence (Huisman *et al.* 2013; Meneveau & Marusic 2013; Stevens *et al.* 2014; de Silva *et al.* 2015, 2017). Figure 1(*b*) shows the normalised second-, fourth- and sixth-order structure
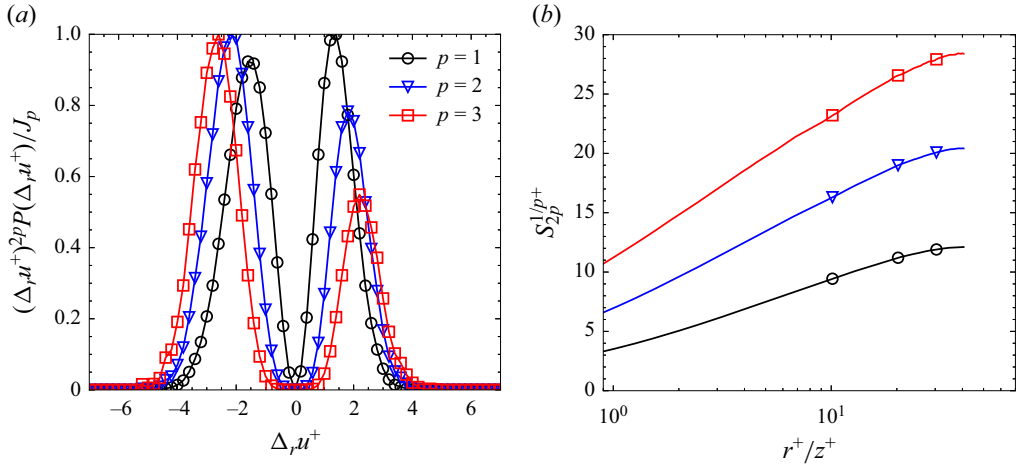
Figure 1. (*a*) Premultiplied p.d.f. of the velocity increment ($\Delta_r u^+ = [u^+(x+r) - u^+(x)]$) at $r^+ \approx 7000$ and $z^+ \approx 825$ for the MBL2 dataset. All the curves in panel (*a*) are normalised by an arbitrary factor J_p such that the maximum is one for all orders. (*b*) Normalised second-, fourth- and sixth-order structure function for the same dataset as panel (*a*) shows the smoothness of the computed structure function. In panel (*b*), r^+ is normalised using z^+ and $S_{2p}^{1/p}$ is normalised using u_τ^2 to facilitate easy comparison with de Silva *et al.* (2015, 2017). This normalisation is not essential for the present scaling (see § 2).

functions for the same dataset, highlighting its smoothness. Similar results were observed for N580, N395 and C590 datasets and are not shown for brevity.

4. Results and discussion

The energy ratio is calculated by computing the slope between normalised structure functions of different orders using a least squares method, similar to the methodology employed by de Silva *et al.* (2017) and Krug *et al.* (2017, 2018). The authors do not explicitly state it as the energy ratio, but from § 4.4, it is evident that their studies are equivalent to the present case. This differs from the extended self-similarity observed in inertial subrange turbulence, where the relative slope of the logarithm of the structure functions exhibits similarity and universality (Benzi *et al.* 1993; Grossmann, Lohse & Reeh 1997). In the present case, the slope is calculated directly, which is the energy ratio.

The rest of this section is dedicated to analysing high-order and low-order structure functions across different flows and at different wall-normal locations. The symbols and labels in the various plots below are summarised in table 2.

4.1. *High-order structure functions*

First, we examine the scaling of the structure functions at locations where the viscous effects are negligible. The viscous effects are negligible in the outer layer (wall-normal locations beyond the velocity maximum) of the vertical buoyancy layer (Maryada *et al.* 2023), and at $z^+ > 2.6\sqrt{Re_\tau}$ for turbulent boundary layers and channels (Wei *et al.* 2005).

Figure 2(*a*) shows E_p^r/E_1^r for all the different datasets. The error bars for SLTEST and MBL1 represent the 95 % confidence interval (de Silva *et al.* 2017). For the rest of the data, the standard deviation of the fit is better or comparable to that of SLTEST and MBL1 and, hence, not shown for clarity. It is evident from the figure that, for all the flows considered, the scaling deviates significantly from (2.5) at higher orders ($2p > 3$), which represents

984 A28-10

Case	Label	Symbol	Wall-normal location	
			$\approx z^+$	$\approx z^+/Re_\tau$
SLTEST	SLTEST	•	1.6×10^4	0.005
MBL1	MBL1	•	800	0.042
N395	N395E	□	180	0.455
MBL2	MBL2V	×	100	0.007
	MBL2W	×	260	0.018
	MBL2L	×	825	0.056
C590	C590B	△	15	0.025
	C590L	▽	76	0.123
	C590H	▽	295	0.5
	C590O	○	530	0.898
N580	N580C	□	60	0.103
	N580E	○	260	0.448
	N580F	◇	405	0.698

Table 2. The wall-normal locations where the longitudinal structure functions were calculated for the different datasets. Here, z^+ corresponds to the wall-normal location in viscous units, while z^+/Re_τ corresponds to the wall-normal location in outer units. The labels and symbols are the same as in figures 2 and 3. See table 1 for details of different cases.
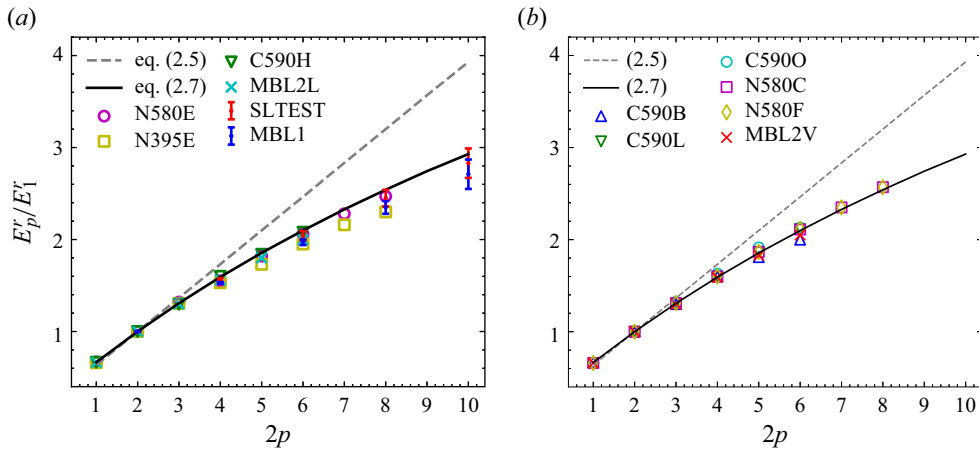

Figure 2. The energy ratio of longitudinal structure functions for different flows. See text and table 1 for details on the different symbols. (*a*) E_p^r/E_1^r of different flows at wall-normal locations where the effect of viscosity is negligible. (*b*) Effect of wall-normal location on E_p^r/E_1^r. Equation (2.5) is the Gaussian scaling and (2.7) is the proposed scaling. See table 2 for a description of the different labels.

the Gaussian scaling. However, it closely follows the scaling in (2.7), which is related to the anomalous scaling of the inertial subrange, demonstrating the efficacy of the proposed scaling.

Having established that the scaling at high orders is universal at moderate Re_τ and at locations where the effects of the wall are minimal, we now investigate the effect of wall-normal location. Figure 2(*b*) shows the scaling of energy ratio for C590, MBL2 and N580 datasets. Viscosity is significant for C590B and MBL2W. It is evident that (2.7)
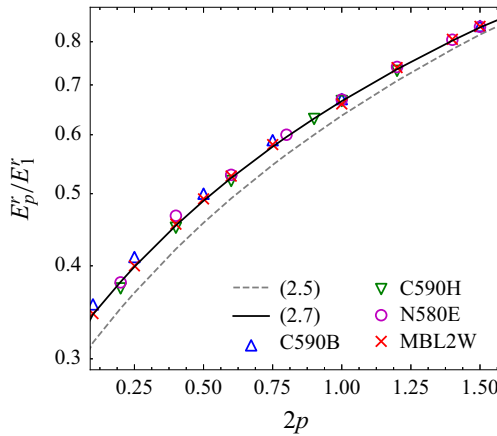
Figure 3. E_p^r/E_1^r for low-order fractional p. See table 2 for a description of the different labels.

correctly predicts the scaling at different wall-normal locations for all the flows considered, even in regions where viscosity is dominant.

The hierarchical scaling is observed for cases N395, N580 and C590, where Re_τ is significantly smaller than that of MBL1, MBL2 and SLTEST, demonstrating that the hierarchical scaling develops at moderate Re_τ even if the asymptotic high-Re_τ behaviour is absent. This was observed by de Silva *et al.* (2017) and Krug *et al.* (2017) in shear-driven wall turbulence for even-order structure functions, but here, we have shown that the scaling is also valid for odd-order absolute structure functions. It is valid even in a buoyancy-driven flow, which is discussed in § 4.3.

Here, it is worth mentioning that (2.7) also holds for C590B, demonstrating that the dynamics of the large scales ($r > L_I$) in the buffer layer in wall turbulence can also be approximated using an additive process. This sub-Gaussian scaling was also observed in Taylor–Couette turbulence (Krug *et al.* 2017), suggesting that (2.7) would correctly predict the scaling even in those situations.

4.2. *Low-order fractional structure functions*

High-order structure functions investigated in § 4.1 represent the tails of the p.d.f.s of the velocity increments. The tails of the p.d.f.s correspond to rare events, and it is not certain that the tails always contain universal effects (Chen *et al.* 2005). The low-order structure functions, however, correspond to the core of the p.d.f.s (common/frequent events). The effects of the rare events, which dominate high-order moments, are insignificant for low-order moments. Therefore, we investigate the scaling of the energy ratio of the fractional moments for $0.1 \leq 2p \leq 1.5$ as it acts as a more stringent measure to test the universality of energy ratio and the validity of (2.7). The scaling of the energy ratio is shown in figure 3, where it is clear that the data follow (2.7) better than (2.5). The deviation from Gaussian scaling for low-order moments is evident for all the flows considered, demonstrating that the anomalous scaling also characterises the fluctuations close to the mean and does not only correspond to rare events. This strongly suggests that the non-Gaussian scaling is present for all the energy-containing fluctuations in shear-dominated flows. Like the inertial subrange, where a transitional behaviour for ζ_n is absent for structure functions of order above and below unity (Sreenivasan *et al.* 1996), transitional behaviour is also not present for the energy ratio.

It should be noted that due to the unavailability of data (precise numerical values) for the MBL1 dataset, it is not shown in figures 2(*b*) and 3. The Re_τ of MBL2 ($Re_\tau \approx 14\,750$) is comparable to MBL1 ($Re_\tau \approx 19\,000$) and, therefore, one should expect quantitatively similar results for the MBL1 dataset.

The scaling of the energy ratio of high-order and low-order structure functions indicates that the energy-containing eddies attain a form of universality in different shear-dominated flows, with the scaling being related to turbulent dissipation. It is again stressed that the present similarity concerns the energy ratio of the eddies and not the eddies themselves.

4.3. *Universality of the energy ratio in a turbulent vertical buoyancy layer*

In figures 2 and 3, it is evident that the universality of the energy ratio observed in turbulent boundary layers and channels is also observed in a turbulent vertical buoyancy layer. As discussed in §3, the vertical buoyancy layer investigated in this study is a buoyancy-driven flow and is substantially different from canonical wall turbulence. In this case, the streamwise velocity variance in the vertical buoyancy layer (vertical convection in general) is produced by both shear and buoyancy (Giometto *et al.* 2017; Maryada *et al.* 2022, 2023; Ke *et al.* 2023). The presence of shear and buoyancy fluxes results in the large-scale eddies being governed by two different processes, in contrast to canonical wall turbulence where only shear is present (Tennekes & Lumley 1972). Therefore, it is not trivial that we observe the present scaling. Despite this, we observe shear-dominated scaling, with the similarity not limited to low-order statistics but also governing intense and rare fluctuations.

Crucially, the strong distance-from-the-wall scaling observed in the logarithmic regions of turbulent boundary layers is not observed in the vertical buoyancy layer (especially in the 'classical regime', i.e. at moderate Re_τ), indicating that the scaling proposed in this study is not limited to attached eddies alone. This, combined with the scaling observed in the viscosity-dominated regions of canonical wall turbulence (see figure 2*b*), again suggests that the physical shape of the eddies is not essential for the energy ratio scaling to hold.

This striking observation of shear-dominated scaling in the vertical buoyancy layer shows that certain vertical convection problems in the 'classical regime' can be analysed using a framework similar to shear-driven flows.

4.4. *Significance of the present hypothesis*

It is worthwhile to briefly discuss the present hypothesis's significance and applicability. First, we examine how the present hypothesis relates to works of de Silva *et al.* (2017) and Krug *et al.* (2017). In those studies, the authors focused on A_p/A_m instead of the energy ratio (the authors specifically focused on A_p/A_1, but the same conclusions hold for different m). From §2.1, we can see that $E_p^r = A_p u_\tau^2$ for the $\ln(r)$ law (2.2), which is valid in the logarithmic region of turbulent boundary layers (Davidson *et al.* 2006*b*; de Silva *et al.* 2015; Chamecki *et al.* 2017). From (2.4), we can write $F_{pm} = A_p/A_m = E_p^r/E_m^r$. Therefore, A_p/A_m and F_{pm} are mathematically equivalent. In figure 2(*a*), SLTEST, MBL1 and MBL2L correspond to the logarithmic region of the turbulent boundary layer, demonstrating that the above relation holds. A consequence of the equivalence of A_p/A_m and F_{pm} is that the present model also provides an elegant solution to the fundamental issue of relating A_p/A_m of wall turbulence to the universal intermittency exponents (de Silva *et al.* 2017).

The previous paragraph implies that the coefficient A_p in the $\ln(r)$ law is related to the energy of the eddies, which is a function of the anomalous scaling exponents of the inertial subrange. De Silva *et al.* (2015) have shown that the structure functions and the one-point moments of streamwise velocity fluctuations are related in the logarithmic region of turbulent boundary layers. Therefore, it is trivial to see that the sub-Gaussian scaling of one-point moments of streamwise velocity fluctuations is also related to the energy ratio, which is related to the intermittent scaling of dissipation. This again highlights a relationship between large and small scales.

5. Concluding remarks and outlook

In summary, we have shown that shear-dominated turbulence attains a hierarchical equilibrium state at large scales ($L_I < r < L_R$) such that the energy ratio of the eddies takes a universal non-Gaussian form. We establish that this is related to the anomalous scaling observed in inertial subrange turbulence (at least for $0.1 \leq 2p \leq 10$), demonstrating a relationship between the large and small scales in shear-dominated flows. A phenomenological model is also proposed to explain this behaviour. By examining data from numerical simulations and experiments, it is shown that the high-order ($2p \geq 2$) and low-order ($0.1 \leq 2p < 2$) energy ratios deviate from Gaussian scaling but closely follow the proposed model, implying that the anomalous scaling is apparent for both rare and frequent events characterising turbulence. The scaling is also valid at different wall-normal locations and under diverse flow conditions, implying that the hierarchical universality of the energy ratio is evident across various turbulent flows so long as shear is dominant. The universality observed is remarkable as it demonstrates that the hierarchical energy equilibrium, as postulated in (2.7), is present and that some form of universality is observed in large scales of shear-dominated turbulence, which are often considered to have significant non-universal effects.

The above observations concerning the correlation between the sub-Gaussian statistics of large scales and the anomalous scaling exponents of inertial subrange turbulence would aid in developing empirical turbulence models that assume a superposition of eddies due to a hierarchical additive process (Marusic & Monty 2019). Another potential application of the present work concerns validating numerical simulations and experiments, which mostly rely on spectra. However, investigating the high-order properties, such as the relative energy density, would be a much more rigorous test to assess the accuracy (Meneveau & Marusic 2013; de Silva *et al.* 2015). Further, this theory can be used to develop scaling theories that relate the generalised scaling of small scales (Benzi *et al.* 1996) to the energy ratio of large scales. This is particularly interesting as it would allow us to develop a more refined picture of intermittency in shear-dominated turbulence, including small and large scales.

Author ORCIDs.
 K.R. Maryada https://orcid.org/0000-0003-3509-0176;
 S.W. Armfield https://orcid.org/0000-0002-8032-0017;

◉ M. MacDonald https://orcid.org/0000-0001-6348-6392;

◉ P. Dhopade https://orcid.org/0000-0003-2011-9300;

◉ S.E. Norris https://orcid.org/0000-0001-5255-8741.

REFERENCES

AGOSTINI, L. & LESCHZINER, M. 2017 Spectral analysis of near-wall turbulence in channel flow at $Re_\tau = 4200$ with emphasis on the attached-eddy hypothesis. *Phys. Rev. Fluids* **2** (1), 014603.

ANDREOLLI, A., GATTI, D., VINUESA, R., ÖRLÜ, R. & SCHLATTER, P. 2023 Separating large-scale superposition and modulation in turbulent channels. *J. Fluid Mech.* **958**, A37.

ARAD, I., L'VOV, V.S. & PROCACCIA, I. 1999 Correlation functions in isotropic and anisotropic turbulence: the role of the symmetry group. *Phys. Rev.* E **59** (6), 6753.

ARMFIELD, S.W., MORGAN, P., NORRIS, S. & STREET, R. 2003 A parallel non-staggered Navier–Stokes solver implemented on a workstation cluster. In *Computational Fluid Dynamics 2002* (ed. S.W. Armfield, P. Morgan & K. Srinivas), pp. 30–45. Springer.

ARNEODO, A., *et al.* 1996 Structure functions in turbulence, in various flow configurations, at Reynolds number between 30 and 5000, using extended self-similarity. *Europhys. Lett.* **34** (6), 411.

ATTILI, A. & BISETTI, F. 2012 Statistics and scaling of turbulence in a spatially developing mixing layer at $Re_\lambda = 250$. *Phys. Fluids* **24** (3), 035109.

BAARS, W.J., HUTCHINS, N. & MARUSIC, I. 2016 Spectral stochastic estimation of high-Reynolds-number wall-bounded turbulence for a refined inner-outer interaction model. *Phys. Rev. Fluids* **1** (5), 054406.

BAARS, W.J., TALLURU, K.M., HUTCHINS, N. & MARUSIC, I. 2015 Wavelet analysis of wall turbulence to study large-scale modulation of small scales. *Exp. Fluids* **56**, 1–15.

BENZI, R., AMATI, G., CASCIOLA, C.M., TOSCHI, F. & PIVA, R. 1999 Intermittency and scaling laws for wall bounded turbulence. *Phys. Fluids* **11** (6), 1284–1286.

BENZI, R., BIFERALE, L., CILIBERTO, S., STRUGLIA, M.V. & TRIPICCIONE, R. 1996 Generalized scaling in fully developed turbulence. *Phys.* D **96** (1–4), 162–181.

BENZI, R., CILIBERTO, S., TRIPICCIONE, R., BAUDET, C., MASSAIOLI, F. & SUCCI, S. 1993 Extended self-similarity in turbulent flows. *Phys. Rev.* E **48** (1), R29.

BIFERALE, L., LOHSE, D., MAZZITELLI, I.M. & TOSCHI, F. 2002 Probing structures in channel flow through SO(3) and SO(2) decomposition. *J. Fluid Mech.* **452**, 39–59.

CASCIOLA, C.M., BENZI, R., GUALTIERI, P., JACOB, B. & PIVA, R. 2001 Double scaling and intermittency in shear dominated flows. *Phys. Rev.* E **65** (1), 015301.

CASCIOLA, C.M., GUALTIERI, P., BENZI, R. & PIVA, R. 2003 Scale-by-scale budget and similarity laws for shear turbulence. *J. Fluid Mech.* **476**, 105–114.

CASCIOLA, C.M., GUALTIERI, P., JACOB, B. & PIVA, R. 2005 Scaling properties in the production range of shear dominated flows. *Phys. Rev. Lett.* **95** (2), 024503.

CHAMECKI, M., DIAS, N.L., SALESKY, S.T. & PAN, Y. 2017 Scaling laws for the longitudinal structure function in the atmospheric surface layer. *J. Atmos. Sci.* **74** (4), 1127–1147.

CHAUHAN, K., PHILIP, J. & MARUSIC, I. 2014 Scaling of the turbulent/non-turbulent interface in boundary layers. *J. Fluid Mech.* **751**, 298–328.

CHEN, S.Y., DHRUVA, B., KURIEN, S., SREENIVASAN, K.R. & TAYLOR, M.A. 2005 Anomalous scaling of low-order structure functions of turbulent velocity. *J. Fluid Mech.* **533**, 183–192.

CHING, E.S.C., SHE, Z.-S., SU, W. & ZOU, Z. 2002 Extended self-similarity and hierarchical structure in turbulence. *Phys. Rev.* E **65** (6), 066303.

CHUNG, D., CHAN, L., MACDONALD, M., HUTCHINS, N. & OOI, A. 2015*a* A fast direct numerical simulation method for characterising hydraulic roughness. *J. Fluid Mech.* **773**, 418–431.

CHUNG, D., MARUSIC, I., MONTY, J.P., VALLIKIVI, M. & SMITS, A.J. 2015*b* On the universality of inertial energy in the log layer of turbulent boundary layer and pipe flows. *Exp. Fluids* **56**, 1–10.

CORRSIN, S. 1958 Local isotropy in turbulent shear flow. *Res. Memo.* 58B11. NACA.

DAVIDSON, P.A. & KROGSTAD, P.Å. 2009 A simple model for the streamwise fluctuations in the log-law region of a boundary layer. *Phys. Fluids* **21** (5), 055105.

DAVIDSON, P.A. & KROGSTAD, P.-Å. 2014 A universal scaling for low-order structure functions in the log-law region of smooth-and rough-wall boundary layers. *J. Fluid Mech.* **752**, 140–156.

DAVIDSON, P.A., KROGSTAD, P.-Å. & NICKELS, T.B. 2006*a* A refined interpretation of the logarithmic structure function law in wall layer turbulence. *Phys. Fluids* **18** (6), 065112.

DAVIDSON, P.A., NICKELS, T.B. & KROGSTAD, P.Å. 2006*b* The logarithmic structure function law in wall-layer turbulence. *J. Fluid Mech.* **550**, 51–60.

Dong, S., Lozano-Durán, A., Sekimoto, A. & Jiménez, J. 2017 Coherent structures in statistically stationary homogeneous shear turbulence. *J. Fluid Mech.* **816**, 167–208.

Dubrulle, B. 1994 Intermittency in fully developed turbulence: Log-Poisson statistics and generalized scale covariance. *Phys. Rev. Lett.* **73** (7), 959.

Frisch, U. 1995 *Turbulence: The Legacy of A. N. Kolmogorov*. Cambridge University Press.

Frisch, U., Sulem, P.-L. & Nelkin, M. 1978 A simple dynamical model of intermittent fully developed turbulence. *J. Fluid Mech.* **87** (4), 719–736.

Ganapathisubramani, B., Hutchins, N., Monty, J.P., Chung, D. & Marusic, I. 2012 Amplitude and frequency modulation in wall turbulence. *J. Fluid Mech.* **712**, 61–91.

Gauding, M., Bode, M., Brahami, Y., Varea, É. & Danaila, L. 2021 Self-similarity of turbulent jet flows with internal and external intermittency. *J. Fluid Mech.* **919**, A41.

Ghannam, K., Katul, G.G., Bou-Zeid, E., Gerken, T. & Chamecki, M. 2018 Scaling and similarity of the anisotropic coherent eddies in near-surface atmospheric turbulence. *J. Atmos. Sci.* **75** (3), 943–964.

Giometto, M.G., Katul, G.G., Fang, J. & Parlange, M.B. 2017 Direct numerical simulation of turbulent slope flows up to Grashof number $Gr = 2.1 \times 10^{11}$. *J. Fluid Mech.* **829**, 589–620.

Grossmann, S., Lohse, D. & Reeh, A. 1997 Application of extended self-similarity in turbulence. *Phys. Rev.* E **56** (5), 5473.

Gualtieri, P., Casciola, C.M., Benzi, R., Amati, G. & Piva, R. 2002 Scaling laws and intermittency in homogeneous shear flow. *Phys. Fluids* **14** (2), 583–596.

Gustenyov, N., Egerer, M., Hultmark, M., Smits, A.J. & Bailey, S.C.C. 2023 Similarity of length scales in high-Reynolds-number wall-bounded flows. *J. Fluid Mech.* **965**, A17.

Huisman, S.G., Lohse, D. & Sun, C. 2013 Statistics of turbulent fluctuations in counter-rotating Taylor–Couette flows. *Phys. Rev.* E **88** (6), 063001.

Hutchins, N., Nickels, T.B., Marusic, I. & Chong, M.S. 2009 Hot-wire spatial resolution issues in wall-bounded turbulence. *J. Fluid Mech.* **635**, 103–136.

Jacobi, I., Chung, D., Duvvuri, S. & McKeon, B.J. 2021 Interactions between scales in wall turbulence: phase relationships, amplitude modulation and the importance of critical layers. *J. Fluid Mech.* **914**, A7.

Jiang, X.-Q., Gong, H., Liu, J.-K., Zhou, M.-D. & She, Z.-S. 2006 Hierarchical structures in a turbulent free shear flow. *J. Fluid Mech.* **569**, 259–286.

Jiménez, J. 1998 Turbulent velocity fluctuations need not be Gaussian. *J. Fluid Mech.* **376**, 139–147.

Ke, J., Williamson, N., Armfield, S.W. & Komiya, A. 2023 The turbulence development of a vertical natural convection boundary layer. *J. Fluid Mech.* **964**, A24.

Kolmogorov, A.N. 1941 The local structure of turbulence in incompressible viscous fluid for very large Reynolds number. In *Doklady Akademii Nauk SSSR*, vol. 30, pp. 301–303.

Kolmogorov, A.N. 1962 A refinement of previous hypotheses concerning the local structure of turbulence in a viscous incompressible fluid at high Reynolds number. *J. Fluid Mech.* **13** (1), 82–85.

Kraichnan, R.H. 1974 On Kolmogorov's inertial-range theories. *J. Fluid Mech.* **62** (2), 305–330.

Kraichnan, R.H. 1991 Turbulent cascade and intermittency growth. *Proc. R. Soc. Lond.* A **434** (1890), 65–78.

Krug, D., Yang, X.I.A., de Silva, C.M., Ostilla-Mónico, R., Verzicco, R., Marusic, I. & Lohse, D. 2017 Statistics of turbulence in the energy-containing range of Taylor–Couette compared to canonical wall-bounded flows. *J. Fluid Mech.* **830**, 797–819.

Krug, D., Zhu, X., Chung, D., Marusic, I., Verzicco, R. & Lohse, D. 2018 Transition to ultimate Rayleigh–Bénard turbulence revealed through extended self-similarity scaling analysis of the temperature structure functions. *J. Fluid Mech.* **851**, R3.

Kunkel, G.J. & Marusic, I. 2006 Study of the near-wall-turbulent region of the high-Reynolds-number boundary layer using an atmospheric flow. *J. Fluid Mech.* **548**, 375–402.

Landau, L.D. & Lifshitz, E.M. 1987 *Fluid Mechanics*, 2nd edn. Pergamon Press.

MacDonald, M. 2022 Direct numerical simulation of momentum and scalar turbulent internal boundary layers. In *23rd Australasian Fluid Mechanics Conference* (ed. C. Lei), p. 302.

Marusic, I. & Monty, J.P. 2019 Attached eddy model of wall turbulence. *Annu. Rev. Fluid Mech.* **51**, 49–74.

Maryada, K.R., Armfield, S.W., Dhopade, P. & Norris, S.E. 2022 Oblique-mode breakdown of the vertical buoyancy layer. *J. Fluid Mech.* **953**, A34.

Maryada, K.R., Armfield, S.W., Dhopade, P. & Norris, S.E. 2023 Large-scale motions in a turbulent natural convection boundary layer immersed in a stably stratified environment. *J. Fluid Mech.* **967**, A40.

Mathis, R., Hutchins, N. & Marusic, I. 2009 Large-scale amplitude modulation of the small-scale structures in turbulent boundary layers. *J. Fluid Mech.* **628**, 311–337.

Meneveau, C. & Marusic, I. 2013 Generalized logarithmic law for high-order moments in turbulent boundary layers. *J. Fluid Mech.* **719**, R1.

Meneveau, C. & Sreenivasan, K.R. 1987 Simple multifractal cascade model for fully developed turbulence. *Phys. Rev. Lett.* **59** (13), 1424.

Motoori, Y. & Goto, S. 2021 Hierarchy of coherent structures and real-space energy transfer in turbulent channel flow. *J. Fluid Mech.* **911**, A27.

Mouri, H., Hori, A., Kawashima, Y. & Hashimoto, K. 2012 Large-scale length that determines the mean rate of energy dissipation in turbulence. *Phys. Rev.* E **86** (2), 026309.

Mouri, H., Hori, A. & Takaoka, M. 2009 Large-scale lognormal fluctuations in turbulence velocity fields. *Phys. Fluids* **21** (6), 065107.

Mouri, H., Takaoka, M., Hori, A. & Kawashima, Y. 2006 On Landau's prediction for large-scale fluctuation of turbulence energy dissipation. *Phys. Fluids* **18** (1), 015103.

Ng, C.S., Ooi, A., Lohse, D. & Chung, D. 2017 Changes in the boundary-layer structure at the edge of the ultimate regime in vertical natural convection. *J. Fluid Mech.* **825**, 550–572.

Obukhov, A.M. 1962 Some specific features of atmospheric turbulence. *J. Geophys. Res.* **67** (8), 3011–3014.

Pan, Y. & Chamecki, M. 2016 A scaling law for the shear-production range of second-order structure functions. *J. Fluid Mech.* **801**, 459–474.

Perry, A.E., Henbest, S. & Chong, M.S. 1986 A theoretical and experimental study of wall turbulence. *J. Fluid Mech.* **165**, 163–199.

She, Z.-S. & Leveque, E. 1994 Universal scaling laws in fully developed turbulence. *Phys. Rev. Lett.* **72** (3), 336.

She, Z.-S. & Waymire, E.C. 1995 Quantized energy cascade and log-Poisson statistics in fully developed turbulence. *Phys. Rev. Lett.* **74** (2), 262.

de Silva, C.M., Krug, D., Lohse, D. & Marusic, I. 2017 Universality of the energy-containing structures in wall-bounded turbulence. *J. Fluid Mech.* **823**, 498–510.

de Silva, C.M., Marusic, I., Woodcock, J.D. & Meneveau, C. 2015 Scaling of second-and higher-order structure functions in turbulent boundary layers. *J. Fluid Mech.* **769**, 654–686.

Sreenivasan, K.R. & Antonia, R.A. 1997 The phenomenology of small-scale turbulence. *Annu. Rev. Fluid Mech.* **29** (1), 435–472.

Sreenivasan, K.R., Vainshtein, S.I., Bhiladvala, R., San Gil, I., Chen, S. & Cao, N. 1996 Asymmetry of velocity increments in fully developed turbulence and the scaling of low-order moments. *Phys. Rev. Lett.* **77** (8), 1488.

Stevens, R.J.A.M., Wilczek, M. & Meneveau, C. 2014 Large-eddy simulation study of the logarithmic law for second-and higher-order moments in turbulent wall-bounded flow. *J. Fluid Mech.* **757**, 888–907.

Tennekes, H. & Lumley, J.L. 1972 *A First Course in Turbulence*. MIT Press.

Toschi, F., Amati, G., Succi, S., Benzi, R. & Piva, R. 1999 Intermittency and structure functions in channel flow turbulence. *Phys. Rev. Lett.* **82** (25), 5044.

Toschi, F., Leveque, E. & Ruiz-Chavarria, G. 2000 Shear effects in nonhomogeneous turbulence. *Phys. Rev. Lett.* **85** (7), 1436.

Townsend, A.A. 1976 *The Structure of Turbulent Shear Flow*, 2nd edn. Cambridge University Press.

Wei, T., Fife, P., Klewicki, J. & McMurtry, P. 2005 Properties of the mean momentum balance in turbulent boundary layer, pipe and channel flows. *J. Fluid Mech.* **522**, 303–327.

Winkelbauer, A. 2012 Moments and absolute moments of the normal distribution. arXiv:1209.4340.

Xie, J.-H., de Silva, C., Baidya, R., Yang, X.I.A. & Hu, R. 2021 Third-order structure function in the logarithmic layer of boundary-layer turbulence. *Phys. Rev. Fluids* **6** (7), 074602.

Yang, X.I.A., Marusic, I. & Meneveau, C. 2016 Hierarchical random additive process and logarithmic scaling of generalized high order, two-point correlations in turbulent boundary layer flow. *Phys. Rev. Fluids* **1** (2), 024402.

Yeung, P.K., Brasseur, J.G. & Wang, Q. 1995 Dynamics of direct large-small scale couplings in coherently forced turbulence: concurrent physical-and Fourier-space views. *J. Fluid Mech.* **283**, 43–95.